CFD Analysis and Risk Management Approach for the Long-Term Prediction of Marble Erosion by Particles Impingement

Gianfranco Caruso[1*], Matteo Mariotti[2], Livio de Santoli[2]

[1] *Dep. DIAEE, Faculty of Industrial and Civil Engineering*
"Sapienza" University of Rome, Italy
[2] *Dep. CITERA, Faculty of Architecture*
"Sapienza" University of Rome, Italy

Abstract

A preliminary study, performed by using a CFD (Computational Fluid Dynamic) analysis, on the erosion of a marble surface generated by particles impingement from air pollutants in indoor or outdoor environments, is presented. To describe the methodology, a very conservative simulation, at low air velocities and particle concentrations, has been carried out by using a commercial CFD computer program, in order to estimate the effect of a long term exposure to this aggressive phenomenon. The Eulerian-Lagrangian approach is used to simulate the gas-solid two-phase flow while semi-empirical model is used to calculate the erosion rate. The case study refers to typical conditions that could occur in an indoor environment, as a museum, but the methodology could be also successfully applied to marble surfaces exposed to the outdoor environment. The marble mass loss due to erosion from impinging particles has been estimated by using results from the CFD analyses and, following the Risk Management approach, the maximum particles concentration giving visible effects in a period of 100 years, for different air velocities and a typical particle distribution of diameters, has been evaluated. The results, obtained using a very conservative model, show that, in the present case study, the detrimental effects on marble surfaces can be controlled and considered negligible.

Keywords: CFD-based erosion model; discrete phase; particles tracking; marble erosion; particles impingement; cultural heritage conservation.

1. Introduction

The installation of HVAC systems in museums needs an appropriate preliminary investigation in order to predict every possible environmental modification, which could be detrimental for the sensible materials of the works of art.

For example, the importance of the statue of David of Michelangelo in Florence (Italy), which in the last decades was submitted to more than 1000000 of visitors per year, focused researchers attention on the implementation of a kind of air ventilation solutions for the preservation of the statue from the action of indoor pollutants. The proposal carried out was related to an air curtain

---

protection system for the statue designed by CITERA Department at the Faculty of Architecture in Rome Error! Reference source not found., with the support of a CFD tool, in order to generate stable environmental condition near the marble surfaces. The simulation results states that the injection of air with a velocity of 1 m/s from the bottom of the statue, with humidity control, and cleaned by an high efficient filtering section, couldn't carry out any kind of decay for the marble of the statue. Nevertheless a study about long term decay phenomena on the marble was carried out in order to evaluate any new possible risk due to the presence of particle pollutants in the air flow surrounding the surface of the statue.

Several CFD simulations using a literature model of erosion ([2], [3]) have been performed, in order to assess long term effects of the particle impingement on marble surfaces. Furthermore, the methodology presented in this paper could be successfully applied to predict also the erosion of marble surfaces exposed to the outdoor environment.

2. Risk Management for air quality controlling in museums

Some researchers, between 1980 and 1990, tried to characterize the effect of pollutants on material with an approach used in risk management [4], [5] based on the concept of dose (the concentration of pollutants multiplied for the duration of the exposure).

This dose is called "Lowest Dose" (LOAED, *Lowest Observed Adverse Effect Dose*) and it is equal to the product of LOAEL and the time in years, being LOAEL (*Lowest Observed Adverse Effect Level*) expressed as the concentration ($\mu g/m^3$) of dispersed pollutant surrounding the object.

The adverse effects must be related to the adopted model of material decaying, that has to be defined, for the specific situation, in terms of concentrations and doses of pollutant substances considered. This decay is a complex function which includes many environmental factors, and also the choices of the physical and chemical characteristics of the material for which is possible to define an adverse effect or a loss of value [6].

According with the reciprocity principle, taking a particular dose of pollutant on a certain object, it is possible to calculate the exposure time needed to make a recognizable decay effect. If, for example, a particular pigment begins to develop to a softer colour when subjected to a dose of 10 $\mu g/m^3$ of SO_2 per year, the average concentration of this substance has to be reduced to less than 1 $\mu g/m^3$ to prevent this colour change in 10 years. An example of this principle is available in the literature [7] and it deals with the making dirty process caused by suspended particulate.

Although it is possible to define the acceptable concentration for every pollutant, this is a very expensive approach, so that many institutions prefer to fix the concentration of the dangerous pollutant for a collection of medium sensibility [8] though this neglects the effect on very sensitive materials.

The higher concentration, experimentally obtained, which doesn't cause adverse modification of the object under certain exposure conditions, in terms of morphology, functional skill, growth, developing, or length of life, is defined as NOAEL, *No Observed Adverse Effect Level*: it is representative of the maximum level for which the damage is not visible in a particular configuration (typology analytical method, exposure elapsed, temperature, presence of other reactive substances). The available information can be very limited, depending on the experimental configuration and they could carry to wrong conclusion about the resistance of the object to the concentration level of a substances. Only an appropriate use of the concept might provide the knowledge of all the parameters needed to make significant this value.

The most conservative situation can be referred to a target of 100 years, as the elapsed time during which the object might not show adverse effect when exposed to the maximum concentration level of the specified pollutant. Maintaining the pollutants concentration under the target level of 1 year could be considered acceptable in some situations, especially if no pollutant source exists in the environment considered.

The approach based on NOAEL and LOAED can represent a starting point to develop a conservation policy which could be applied to every Institution.

In the framework of the activities performed to analyze possible ventilation solutions for the preservation of a marble statue from the action of indoor pollutants, a study about long term decay phenomena on the marble has been carried out, in order to evaluate any new possible risk due to the presence of particulate in the air flux surrounding the surface of the statue and to assess long term effects of the impingement on marble surfaces.

This parametric study, based on CFD simulations and the Tulsa model of erosion ([2], [3]), has been performed at low air velocities and particle concentrations, typical in an indoor environment, but it could also applicable in outdoor situations.

3.   Numerical details

A commercial CFD code (FLUENT 6.3.26) has been used for the Lagrangian simulation of confined gas-particle flow. The Lagrangian method is based on a continuum model for gas phase and a discrete method for particulate phase. The CFD code solves the governing equations of gas flow by a finite-volume formulation on a non-orthogonal, curvilinear coordinate grid system using a collocated variable arrangement. The SIMPLEC algorithm resulting in a set of algebraic equations, which are solved using a line-by-line tridiagonal matrix algorithm, achieves pressure/velocity coupling. A k– standard turbulence model has been chosen to model gas turbulent fluctuations. A Lagrangian-formulated particle equation of motion is solved via an advanced Runge–Kutta method to predict particle velocity and trajectories once the gas flow field is obtained. The software can use also a stochastic method that incorporates the instantaneous values of gas velocity including fluctuation components appearing in the equation of particle motion, which are typical of turbulent behaviour.

3.1. Particles tracking

The trajectory of a discrete phase particle (or droplet or bubble) is predicted by integrating the force balance on the particle, which is written in a Lagrangian reference frame [11]. This force balance equates the particle inertia with the forces acting on the particle, and can be written (for the x direction in Cartesian coordinates) as:

$$\frac{du_p}{dt} = F_D + \frac{g_x \left(\cdots_p - \cdots \right)}{\cdots_p} + F_x \qquad\qquad 1$$

where u is the fluid phase velocity, u_p is the particle velocity, $\cdots$ is the fluid density, $\cdots_p$ is the density of the particle, and d_p is the particle diameter, F_x is an eventual additional acceleration (force/unit particle mass) term, F_D is the drag force per unit particle mass:

$$F_D = \frac{18 \cdot \sim}{d_p^2 \cdot \cdots_p} \cdot \frac{C_D \cdot \mathrm{Re}}{24} \cdot \left(u - u_p \right) \qquad\qquad 2$$

Re is the relative Reynolds number, which is defined as

$$\mathrm{Re} = \frac{\cdots \cdot d_p \cdot \left| u - u_p \right|}{\sim} \qquad\qquad 3$$

where $\sim$ is the viscosity of the fluid, The drag coefficient, C_D, can be taken from either:

$$C_D = a_1 + \frac{a_2}{\mathrm{Re}} + \frac{a_3}{\mathrm{Re}^2} \qquad\qquad 4$$

where a_1, a_2, and a_3 are constants that apply to smooth spherical particles over several ranges of Re given by Morsi and Alexander [17], or:

$$C_D = \frac{24}{\mathrm{Re}} \cdot \left(1 + b_1 \cdot \mathrm{Re}^{b_2}\right) + \frac{b_3 \cdot \mathrm{Re}_{sph}}{b_4 + \mathrm{Re}_{sph}}$$ 5

where, according to Haider and Levenspiel [10]:

$$b_1 = e^{2.3288 - 6.4581\{ + 2.4486\{^2}$$ 6

$$b_2 = 0.0964 + 0.5565\{$$ 7

$$b_3 = e^{4.905 - 13.8944\{ + 18.422\{^2 - 10.2599\{^3}$$ 8

$$b_4 = e^{1.4681 + 12.2584\{ - 20.7322\{^2 + 15.8855\{^3}$$ 9

The shape factor, $\{$, is defined as

$$\{ = \frac{s}{S}$$ 10

where s is the surface area of a sphere having the same volume as the particle, and S is the actual surface area of the particle. The Reynolds number Re_{sph} is computed with the diameter of a sphere having the same volume.

For sub-micron particles, Stokes' drag law is also applicable but, in this case, F_D is defined as

$$F_D = \frac{18 \cdot \sim}{d_p^2 \cdot \cdots_p \cdot C_C} \cdot \left(u - u_p\right)$$ 11

The factor C_C is the Cunningham correction to Stokes' drag law , which it is computed from

$$C_C = 1 + \frac{2 \cdot \}}{d_p}\left(1.257 + 0.4e^{-\left(1.1d_p/2\}\right)}\right)$$ 12

where $\}$ is the molecular mean free path.

Upon striking a wall surface, a particle is forced to rebound according to the prescribed restitution coefficients. In order to accurately predict the particle trajectories, an appropriate rebound model describing the particle–wall collision must be used. At impact, the reflected velocity of the particle is lower than the incoming velocity due to energy transfer. This impact signature is described by the momentum-based coefficient of restitution, *e*. Researchers have shown that the particle incoming angle may have a significant effect on the coefficient of restitution. Grant and Tabakoff [12] and Sommerfeld [13][14] treated the rebound dynamics of the particles in a statistical sense. Based on experimental data (for 2024 Aluminum and 200 μm sand particles), Grant and Tabakoff postulated the mean values of the coefficients of restitution for perpendicular and parallel velocity components (e_{per} and e_{par}), which are incoming angle-dependent (Γ) distributions [12], Fig. 1:

$$e_{per} = 0.993 - 1.76Γ + 0.56Γ^2 - 0.49Γ^3$$ 13

$$e_{par} = 0.998 - 1.66Γ + 2.11Γ^2 - 0.67Γ^3$$ 14

Particle fragmentation and/or particle rotation are not considered. By tracking a statistically significant number of particles, overall pictures of the mean particulate flow field can be obtained based on the concept of conservation. The mean velocity and concentration of incident and reflected particles near wall surface can also be estimated from particle trajectories. More details about the CFD models used can be found in the FLUENT code documentation [11].
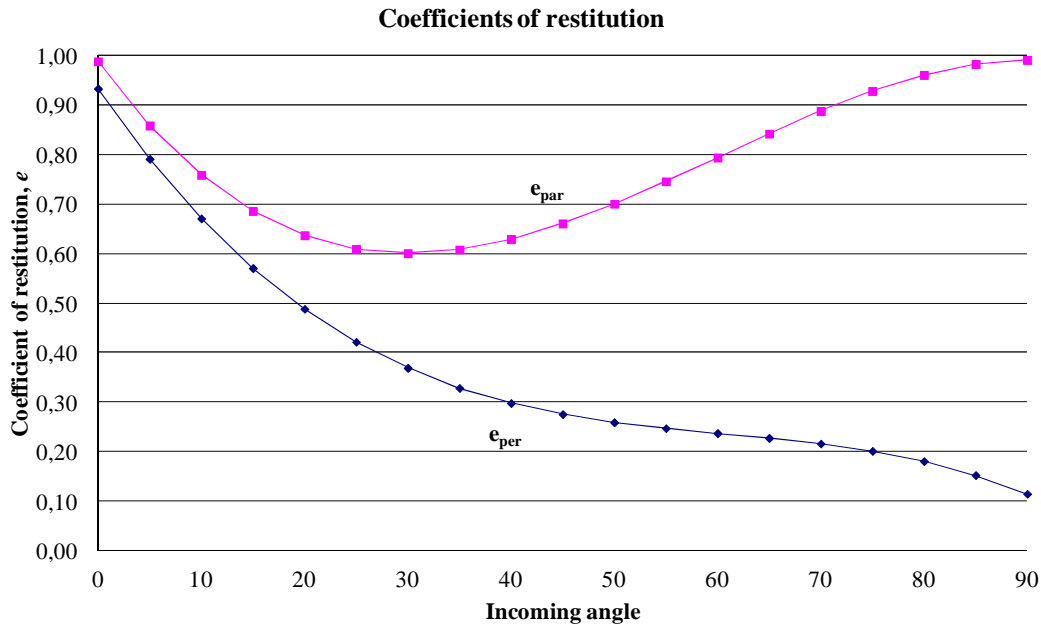

Figure 1. Mean values of coefficients of restitution, according to [12]

3.2. Erosion model

The erosion rate is defined as the mass loss of the wall due to erosion divided by the mass of particles impacting the wall. The erosion ratio depends on the particle impact speed and impact angle.

According to Edwards et al. [2], [15] and Salama et al. [16], [17], the erosion rate (E_R) expressed in kg/(m^2 s) is defined as:

$$E_R = \sum_{p=1}^{N} \frac{\dot{m}_p \cdot C\left(d_p\right) \cdot f\left(\ \right) \cdot v^{b(v)}}{A} \qquad 15$$

where $b(v)$ is an exponent ranging from 1.5 to 2.6, depending on velocity v, and A is the impingement area. The function $C\left(d_p\right)$ depends on the shape of the particles and on the hardness of the impinged material; it is defined by the expression:

$$C\left(d_p\right) = 470.22 \cdot B^{-0.59} \cdot F_s \qquad 16$$

where B is the Brinel hardness of the material stroked by particles, and F_s is a shape coefficient for particles, which can be 0.2, 0.5 or 1 depending on the shape of particles which can be respectively rounded, semi-rounded or sharp.

The angle function $f\left(\Gamma\right)$ describes the dependence on the impact angle Γ, which is 0 when the trajectory is perpendicular to the surface, and is 90° when the particle impinges tangentially. This normalized function can be expressed by:

$$f(r) = \frac{-0.384 \cdot r^2 + 0.227 \cdot r}{0.039} \quad \text{when } r \leq 15°$$

17

$$f(r) = \frac{0.03147 \cdot \cos^2 r \cdot \text{sen} r + 0.003609 \cdot \text{sen}^2 r}{0.039} \quad \text{when } r > 15°$$
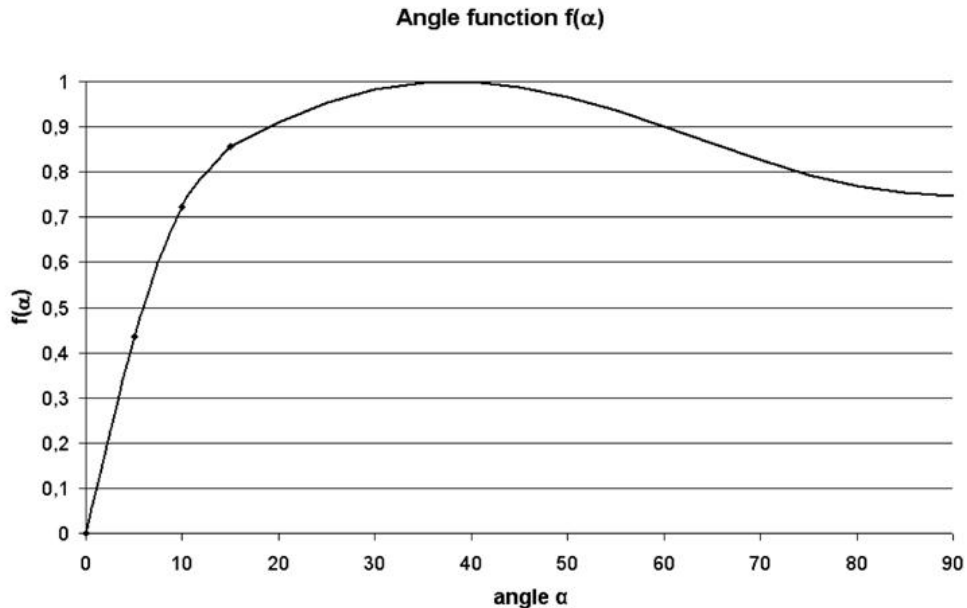
as shown in Fig. 2.

Angle function f(α)

Figure 2. Impingement angle function in the erosion model

4. Hardness of marble

The expression of the erosion ratio (eq. 15) represents the amount of material, with a specified Brinel hardness, lost per unit of time and area, and the model described was originally developed for metal piping. As the Brinell hardness is related only to metals, it is very difficult to find a trustworthy value for marble. Indeed hardness for stony material is given by the Mohs scale or, more recently, the sclerometer scale. This aspects could be considered a weak point in the application of this methodology and further analyses and experimental data should be obtained in the future.

In mineralogy the property of matter is commonly described as the resistance of a substance to being scratched by another substance. In metallurgy hardness is defined as the ability of a material to resist plastic deformation. The Brinell hardness tests determine the depth which a ball or cone will penetrate into the metal, under a given load, within a specific period of time. In a different way, Mohs hardness for stony materials is a rough measure of the resistance of a smooth surface to scratching or abrasion, expressed in terms of a scale defined by the German mineralogist Friedrich Mohs (1812). The Mohs hardness of a mineral is determined by observing whether its surface is scratched by a substance of known or defined hardness. To give numerical values to this physical property, minerals are ranked along the Mohs scale (Table 1), which includes 10 minerals having arbitrary hardness values.

In Table 2 [18] other materials that approximate the hardness of some reference minerals are shown. As indicated by the ranking in the scale, if a mineral is scratched by orthoclase but not by apatite, its Mohs hardness is between 5 and 6.

TABLE 1: A COMPARISON OF MOHS SCALE WITH ABSOLUTE HARDNESS BY A SCLEROMETER

Hardness (mohs)	Mineral	Absolute Hardness (sclerometer)
1	Talc ($Mg_3Si_4O10(OH)_2$)	1
2	Gypsum ($CaSO_4 \cdot 2H_2O$)	2
3	Calcite ($CaCO_3$)	9
4	Fluorite (CaF_2)	21
5	Apatite ($Ca_5(PO_4)_3(OH\text{-},Cl\text{-},F\text{-})$)	48
6	Orthoclase Feldspar ($KAlSi_3O_8$)	72
7	Quartz (SiO_2)	100
8	Topaz ($Al_2SiO_4(OH\text{-},F\text{-})_2$)	200
9	Corundum (Al_2O_3)	400
10	Diamond (C)	1500

In the determination procedure it is necessary to be sure that a scratch is actually made and not just a "chalk" mark that will rub off. For this reason the Mohs test, while greatly facilitating the identification of minerals in the field, is not suitable for accurately gauging the hardness of industrial materials such as steel or ceramics. (For these materials a more precise measure is to be found in the Vickers hardness or Knoop hardness). Another disadvantage of the Mohs scale is that it is not linear; that is, each increment of one in the scale does not indicate a proportional increase in hardness. For instance, the progression from calcite to fluorite (from 3 to 4 on the Mohs scale) reflects an increase in hardness of approximately 25 percent; the progression from corundum to diamond, on the other hand (9 to 10 on the Mohs scale), reflects a hardness increase of more than 300 percent.

TABLE 2: MOHS HARDNESS OF METALS [18]

Hardness (mohs)	Mineral
2.5	Fingernail
2.5-3	**Gold, Silver**
3	Copper penny
4-4.5	Platinum
4-5	Iron
5.5	Knife blade
6-7	Glass
6.5	Iron pyrite
7+	Hardened steel file

Even though the Mohs scale was defined for stony materials, the value for some soft metals as gold, platinum or silver can be found in the literature (Table 2). Finding that gold has approximately the same hardness of marble (which, according to Hoigart [19], is 3), and comparing the metal and the stone scale, the Brinel hardness value for the marble, in the present analyses, equal to the value for gold, 120 kg/mm^2, in order to use the above described erosion model (equations 15 and 16).

5.   Model geometry and assumptions

The CFD-based erosion prediction procedure has been performed on a marble cylinder with a diameter of 0.3 m in a 0.9 m width rectangular duct, subjected to different air flow velocities (0.1, 0.5, 1 and 2 m/s) and pollutants concentration (100, 250, 500, 1000 and 10000 µg/m³). In Fig. 3 the geometry and a typical velocity field are shown.

A structured 2D grid has been adopted with a density, after a grid refinement process, of 10 mm at inlet (90 meshes along the inlet boundary) and a refinement up to 1 mm pitch near the cylinder surface (Fig. 4).

Three different diameters of particles have been chosen in the mixture, in order to better simulate the characteristic distribution of air pollutants in indoor environments. Accordingly to a typical environment, a 50% PM_{10}, 35% $PM_{2.5}$ and 15% $PM_{0.5}$ distribution [20] has been used.
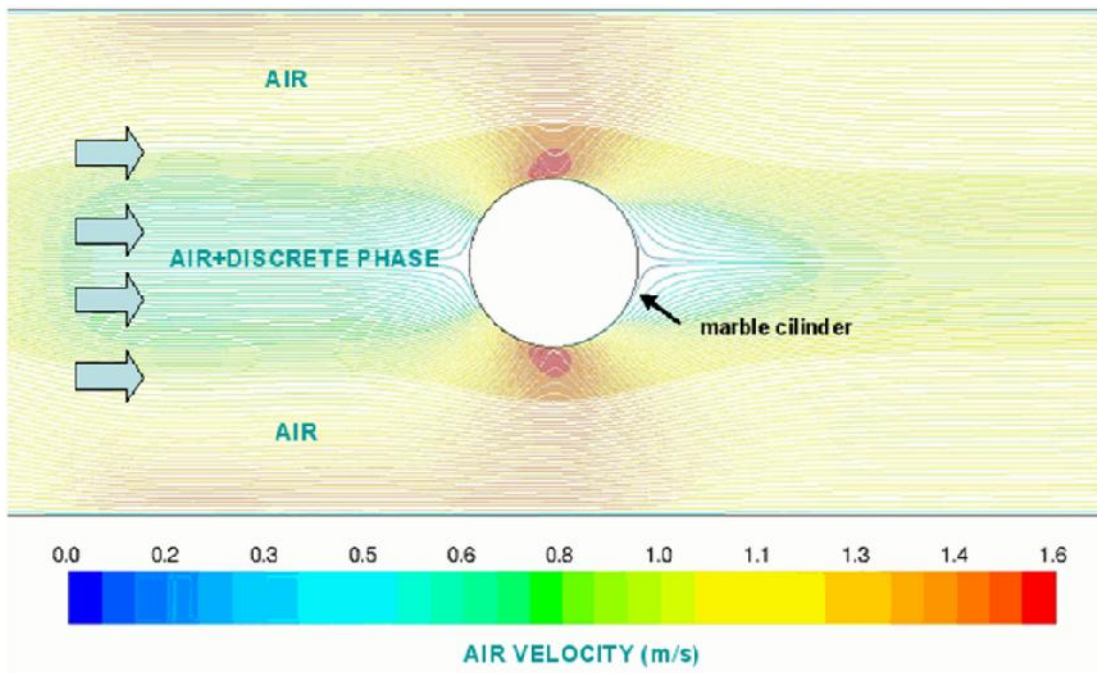

Figure 3. Geometry and air flow pathlines coloured by velocity (inlet $v = 1$ m/s)
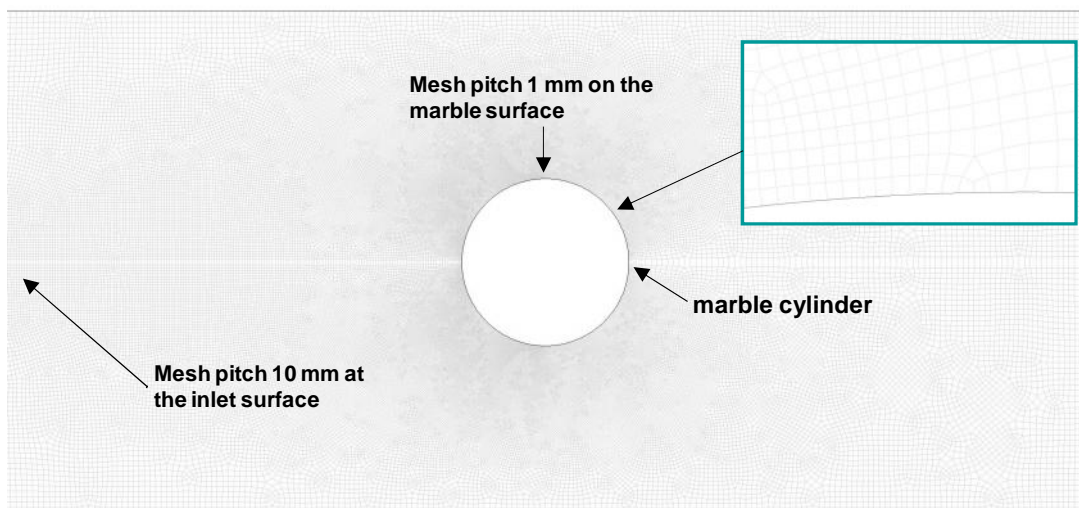

Figure 4. Structured mesh adopted

The stochastic particle–wall collision rebound model is used to predict the erosion. A total of 3000 sand particles are released randomly at the inlet of the duct to represent the particles mass flow rate. The number of particles is not very large, but it appears, by the support of some sensitivity analyses, sufficient to simulate the phenomenon,.

Gas-particle two-phase flows are characterized by a strong coupling between the phases. However, it is well known that if concentration of particles is relatively small, the gas flow field is not significantly influenced by the presence of particles. Computations with one-way coupling can yield quite accurate results for dilute gas-particle flows, such as in the present work.

6. Results and discussion

The surface decay of the cylinder is evaluated trough the erosion rate (kg/m^{2}s) in order to measure the loss of material due to the impingement of particles. Knowing the erosion rate and fixing an evaluation elapsed time, the thickness of material loss on marble surface can be estimated.

Fig. 5 shows an example of the erosion rate on the specimen contour and in Fig. 6 some particle traces are evidenced, close to the side surface of the cylinder.
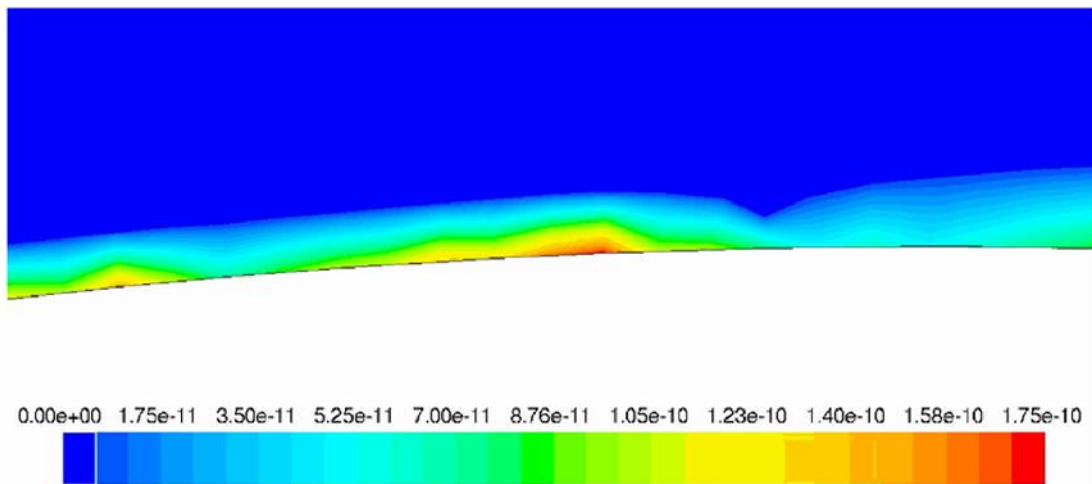

0.00e+00 1.75e-11 3.50e-11 5.25e-11 7.00e-11 8.76e-11 1.05e-10 1.23e-10 1.40e-10 1.58e-10 1.75e-10
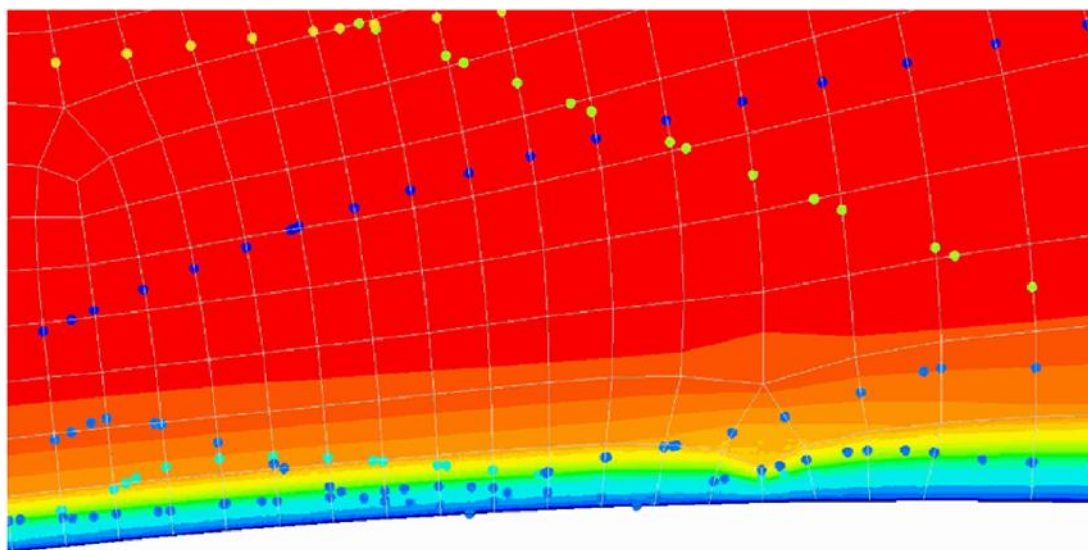
Figure 5. Erosion rate in kg/m^{2}s

Figure 6. Example of particles tracking in the simulations

In Table 3, the erosion rates obtained for an air-particles mixture velocity of 1 m/s are reported. The results refers to the average values on the front part of the specimen (directly exposed to the particles flux) and on the rear zone of the cylinder. The maximum erosion rates (occurring in the main impact area of the frontal region of the cylinder) is also reported in the table; the maximum values are four times higher than the averaged ones, but they have to be considered only as indicative values, being these strongly depending on the calculation mesh, and could be affected by a large numerical uncertainty.

TABLE 3: AVERAGE EROSION RATES AT $v = 1$ m/s

Particle concentration ($\sim$g/m^3)	Avg. E_R on front surface (kg/m^{2}s)	Avg. E_R on rear surface (kg/m^{2}s)	Max E_R (kg/m^{2}s)
10000	$3.901\ 10^{-10}$	$2.407\ 10^{-10}$	$1.575 10^{-9}$
1000	$4.851\ 10^{-11}$	$2.257\ 10^{-11}$	$1.858 10^{-10}$
500	$2.819\ 10^{-11}$	$1.027\ 10^{-11}$	$1.002 10^{-10}$
250	$1.358\ 10^{-11}$	$5.305\ 10^{-12}$	$4.430 10^{-11}$
100	$6.040\ 10^{-12}$	$2.234\ 10^{-12}$	$1.891 10^{-11}$

An erosion thickness of 10 μm can be considered as the "*lowest observed adverse effect*" for marble erosion, being this value the smallest size visible by the human eye. Assuming this value, the LOAED can be calculated from the erosion rate and the marble density (2400 kg/m^3), obtaining a value of 15100 μg/m^{3}yr, for the air-particle mixture velocity of 1 m/s, (Fig. 7), considering the average erosion rate on the front zone of the specimen.

Assuming a target of 100 yr as the exposure time during which the major part of object might not show adverse effect, the NOAEL can be evaluated. As shown in Table 4, the particle concentration for which the eroded thickness is lower than 10 μm is in the range 100-200 μg/m^3.

In the same Table 4 and in Fig. 7 the results for different flow velocities and concentrations are shown: if the flow velocity is reduced to 0.5 m/s, the NOAEL is in the range 700-800 μg/m^3, to observe an average erosion of 10 μm in 100 years and, on the contrary, a concentration of only 20 μg/m^3 is needed to avoid long term adverse effects on the surface, if air velocity raises to 2 m/s.
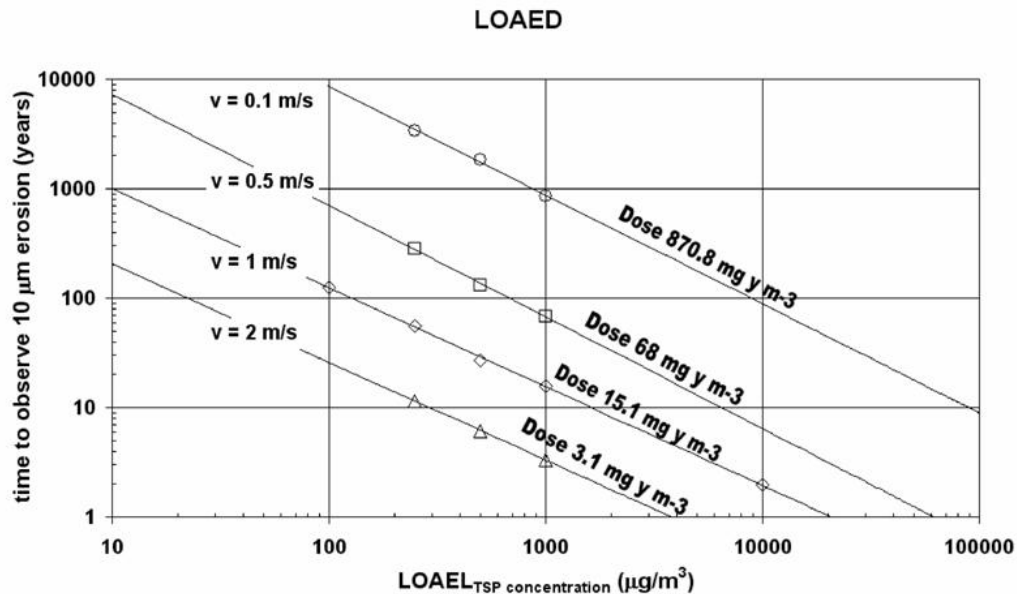

Figure 7. Calculated LOAD for different air-particles velocity

TABLE 4: EROSION THICKNESS AFTER 100 YEARS

Particle concentration (~g/m^3)	v = 0,1 m/s Erosion after 100 yr (~m)	v = 0,5 m/s Erosion after 100 yr (~m)	v = 1 m/s Erosion after 100 yr (~m)	v = 2 m/s Erosion after 100 yr (~m)
10000			512	
1000	1.2	14.5	64	303
500	0.5	7.5	37	163
250	0.3	3.5	18	87
100			8	

7. Conclusions

A study about long term decay of a marble surface has been developed, by using a CFD-based erosion model, in order to evaluate any possible risk due to the presence of particulate in the air flux surrounding the surface of a marble statue. Several erosion models in the literature were developed and validated especially for metallic surfaces, as many engineering industries, such as the oil and gas industry, have the need to transport fluids with entrained solid particles. In this paper, an attempt to apply these models to evaluate the detrimental effects deriving from particulate in air flows on marble surfaces has been performed. A parametric study, with low air velocities and low particles concentrations, typical of an indoor environment, has been carried out, but the methodology could be applied also for higher velocities and pollutants concentrations, as in an outdoor environment. Following the Risk Management approach, the LOAEL (*Lowest Adverse Effect Level*) as a function of different particles concentrations and a typical indoor particle distribution of diameters and the NOAEL (*No Observed Adverse Effect Level*) have been estimated. The results, obtained using a very conservative model, show that this decay effect on marble surfaces could be controlled and considered negligible in this specific application, but long term effects could be evidenced with air velocities and particulate concentrations higher than the typical values in a protected indoor environment.

Nomenclature

$a_{1...}a_3$	constants in eq. 4	*Re*	relative Reynolds number, eq. 3
A	Impingement area, m^2	*s, S*	particle surface area, m^2
$b_{1...}b_4$	parameters in eq. 5	*u*	velocity, m/s
B	Brinell hardness	*v*	particle impact velocity, m/s
$b(v)$	velocity exponent in eq. 15		
$C(d_p)$	hardness function in eq. 15	*Greek symbols*	
C_D	drag coefficient	Γ	impinging angle
C_C	Cunningham factor in eq 12	$\}$	molecular mean free path, m
d_p	particle diameter, m	$\sim$	dynamic viscosity, kg/ms
e	coefficient of restitution, eqs. 13-14	$...$	density, kg/m^3
E_R	erosion rate, kg/m^{2}s		shape factor
$f(\Gamma)$	normalized angle function, eq. 17		
F_D	drag force per unit particle mass, m/s^2	*Suffixes*	
F_x	additional forces per unit mass, m/s^2	p	particle
$\dot{m}_p$	particles mass flow rate, kg/s	par, per	parallel, perpendicular

Acknowledgement

This study is included in a research on the "Protection of the David from air pollutants" commissioned by the Polo Museale Fiorentino to which the authors are grateful for their encouragement to this work.

References

[1]   de Santoli L., Mancini F., Mariotti M., *Air curtains as a protection for indoor cultural heritage: a proposal for Michelangelo's David in Florence*. In *10th Int. Conf. on Indoor Air Quality and Climate, 4-9 September 2005*. 2005. Beijing.

[2]   Edwards J.K., McLaury B. S., Shirazi S. A., *Modeling Solid Particle Erosion in Elbows and Plugged Tees*, J. of Energy Resources Technology, 2001. **123**: p. 277-284.

[3]   Chen X., McLaury B. S., Shirazi S. A., *Application and experimental validation of a computational fluid dynamics (CFD)-based erosion prediction model in elbows and plugged tees*, Computers & Fluids, 2004. **33**: p. 1251-1272.

[4]   ACS (American Chemical Society) and Resource for the Future, Understanding Risk Analysis. In www.rff.org/misc_docs/risk_book

[5]   de Santoli L. Caruso G., Risk Management per i beni culturali. CDA Condizionamento dell'aria, riscaldamento e refrigerazione, 2006. **3**: p. 46-50.

[6]   Ashley-Smith J., Risk Assessment for Object Conservation. Oxford, Butterworth-Heinemann, 1999.

[7]   Nazaroff W.W., Ligoki M.P., Salmon L.G. et al., Protection of Work of Art from Soiling due to Airborne Particulate. GCI Scientific Program Report, Marina del rey, The Getty Conservation Institute, 1992.

[8]   ASHRAE Application, Museums, Libraries, and Archives, Atlanta: American Society of Heating, Refrigerating and Air-conditioning Engineers, Inc., 1999, 20.1-20.13

[9]   Morsi S. A. and Alexander A. J., *An Investigation of Particle Trajectories in Two-Phase Flow Systems*, J. Fluid Mech., 1972. **55**(2): p. 193-208.

[10]   Haider A. and Levenspiel O., *Drag Coefficient and Terminal Velocity of Spherical and Nonspherical Particles*, Powder Technology, 1989. **58**: p. 63-70.

[11]   FLUENT 6.3 Documentation (Ansys), 2006

[12]   Grant T, Tabakoff W. *Erosion prediction in turbomachinery resulting from environmental solid particles.* J Aircraft, 1975. **12**: p. 471–547.

[13]   Sommerfeld M., *Modeling of particle–wall collisions in confined gas-particle flows.* Int J Multiphase Flow, 1992. **18**: p. 905–26.

[14]   Sommerfeld M., *Particle–wall collisions: experimental studies and numerical models*. ASME FED, 1993. **166**: p. 183–191.

[15]   Edwards J. K., McLaury B. S., Shirazi S. A., *Evaluation of Alternative Pipe Bend Fittings in Erosive Service*, In *Proceedings of ASME Fluids Engineering Division Summer Meeting*, Boston, June 2000.

[16]   Salama M. M., Venkatesh E. S., *Evaluation of api rp14e erosional velocity limitations for offshore gas wells*, In *Proceedings of OTC Conference*, pp. 371-376, Houston, May 1983

[17]   Salama, M., *Influence of Sand Production on Design Operations of Piping Systems*, in Corrosion 2000, 2000.

[18]   American Federation of Mineralogical Societies, Inc., Web site http://www.amfed.org/t_mohs.htm

[19]   Hoigard K. R., Dimension Stone Cladding: Design, Construction, Evaluation, and Repair, p.34, ASTM, 2000.

[20]   de Santoli L., Fracastoro G. La qualità dell'Aria negli Ambienti Confinati, Collana Aicarr, 2000, p. 32.